Published online 8 September 2006 *Nucleic Acids Research, 2006, Vol. 34, No. 16* ***4609–4621***
doi:10.1093/nar/gkl640

The *Drosophila G9a* gene encodes a multi-catalytic histone methyltransferase required for normal development

Marianne Stabell, Ragnhild Eskeland[1], Mona Bjørkmo, Jan Larsson[2], Reidunn B. Aalen, Axel Imhof[1] and Andrew Lambertsson*

Department of Molecular Biosciences, University of Oslo, PO Box 1041, Blindern, NO-0316 Oslo, Norway, [1]Adolf-Butenandt Institute, Department of Molecular Biology, Histone Modifications Group and Protein Analysis Unit, Ludwig-Maximillians University of Munich, Schillerstrasse 44, DE-80336 Munich, Germany and [2]UCMP, Umeå University, SE-901 87 Umeå, Sweden

Received June 6, 2006; Revised July 24, 2006; Accepted August 17, 2006

ABSTRACT

Mammalian G9a is a histone H3 Lys-9 (H3–K9) methyltransferase localized in euchromatin and acts as a co-regulator for specific transcription factors. G9a is required for proper development in mammals as *g9a*$^{-}$/*g9a*$^{-}$ mice show growth retardation and early lethality. Here we describe the cloning, the biochemical and genetical analyses of the *Drosophila* homolog dG9a. We show that dG9a shares the structural organization of mammalian G9a, and that it is a multi-catalytic histone methyltransferase with specificity not only for lysines 9 and 27 on H3 but also for H4. Surprisingly, it is not the H4–K20 residue that is the target for this methylation. Spatiotemporal expression analyses reveal that dG9a is abundantly expressed in the gonads of both sexes, with no detectable expression in gonadectomized adults. In addition we find a low but clearly observable level of dG9a transcript in developing embryos, larvae and pupae. Genetic and RNAi experiments reveal that dG9a is involved in ecdysone regulatory pathways.

INTRODUCTION

Modifications of histones are an important mark for transcriptional regulation during embryonic development. The protruding tales of the histones are modified by acetylation, phosphorylation, ubiquitination and arginine and lysine methylation, and the combinations are hypothesized to form a histone code (1,2). The best-characterized substrates for lysine methylation in eukaryotic cells are histone proteins, although methylation of several non-histone proteins, such as the tumor suppressor p53, has been reported as well (3).

Histone H3 has been shown to be methylated on lysine residues K4, K9, K27, K36 and K79 whereas in histone H4, K20 is methylated (4,5). Each of these lysine side chains can be mono-, di- or tri-methylated by histone lysine methyltransferases (HKMTases), which, except for Dot1 (6), carry a catalytic SET [Su(var), Enhancer of Zeste, Trithorax] domain (7). The SET domain is a conserved ~130 amino acid sequence, which is flanked by the less conserved pre-SET and post-SET regions at the amino and C-termini, respectively. The specificity of a HKMTase, as well as the number of methyl residues that attaches to a lysine residue, depends on the structure of the HKMTase or the presence of additional co-factor proteins (8). On the other hand Ezh2 requires the presence of the co-factors suppressor of zeste-12 (SUZ12) and embryonic ectoderm development (Eed) for tri-methylation of H3–K27 (9). The HKMTase ERG-associated protein (ESET) di-methylates H3–K9, but is converted into a tri-methylating enzyme by its association with a mouse-activating transcription-factor-associated modulator (mAM) (10). The methylated histones recruit proteins that carry CHROMO, TUDOR or WD40 domains and are capable of specific interactions with differently methylated lysine residues reviewed in Ref. (11). This recruitment step is likely to define a unique functional readout for individual lysine methylations. Thus, tri-methylation of lysine 9 in histone H3 by Suv39H1 and Suv39H2 creates a binding site for the chromodomain-containing heterochromatic protein HP1 which is thought to induce heterochromatin formation (12). Di-methylation of H3–K9 by G9a is associated with the silencing of euchromatic genes (13).

Mammalian G9a mono- and di-methylates H3–K9 at euchromatic loci (14,15), and has recently also been found at heterochromatic loci (16). In g9a^{-}/g9a^{-} mice H3–K9

*To whom correspondence should be addressed. Tel: +47 22 85 48 94; Fax: +47 22 85 47 26; Email: g.a.lambertsson@imbv.uio.no
Present address:
Mona Bjørkmo, The Biotechnology Centre of Oslo, University of Oslo, NO-0317 Oslo, Norway

methylation is drastically reduced resulting in severe growth retardation and early lethality (17). The loss of G9a primarily affects the methylation of H3–K9 in euchromatic regions (14). G9a is the major euchromatic histone H3–K9 methyltransferase in higher eukaryotes but in *Drosophila* the euchromatic H3–K9 HKMTase has not been characterized. Although the H3–K9 methylation is strongly reduced in *Su(var)3–9* null mutants, a small amount of H3 molecules remain methylated at K9 suggesting the existence of other K9 specific HKMTases in *Drosophila* (18).

There are several reports demonstrating the silencing effects from H3–K9 methylation, including the inactive X chromosome of female mice and humans (19), and developmentally regulated genes (20).

In a search for SET domain containing genes in *Drosophila* that might code a K9 specific HKMTase, we performed a bioinformatics search of the *Drosophila melanogaster* genome and found the gene *CG2995* which share significant homology to mammalian *G9a*. In this paper we describe the cloning, and the biochemical and genetical analyses of *CG2995*. We show that it encodes a histone methyltransferase specific for H3–K9, K27 and H4, and that it shares the structural organization of mammalian G9a. Therefore, we suggest that CG2995 is renamed *dG9a*. It adds up to three methyl groups to unmethylated H3 and H4. Our results indicate a role for *dG9a* in germ cell formation. Using RNAi we show that *dG9a* is critical for development, very likely by being involved in the ecdysone regulated gene expression.

MATERIALS AND METHODS

Fly handling and generation of transgenic flies

All genetic crosses were carried out at 25°C. Fly lines were obtained from the Bloomington *Drosophila* stock centre.

Generation of double stranded (ds) RNA was performed by using the pHIBS and pUds-GFP vectors as described in Ref. (21). A 756 bp fragment of *dG9a* cDNA was PCR amplified with the 2995UBamHI (5′-CAAGGATCCTGTCGCACTTCTCGTTCATC-3′) and 2995LKpnI (5′-TGCGGTACCTGCTGGATAATGCATTGTGTT-3′) primers.

Transgenic flies were generated by P-element mediated transformation, and nine independent lines on different chromosomes were established, including the 2995-18 line used in this study. The GAL4-UAS system (22) was used to express dG9a.IR construct, and *Act5C-GAL4* (BL 4414), *da-GAL4* (BL 5460), *P{GawB}c698a* (BL 3739), and *ap-GAL4* (BL 3041) were used as drivers. As control the 2995-18 line without driver was used.

The *ap-GAL4,UAS-dG9a.IR/EcR*^{M554fs} flies were generated by standard genetic procedures.

Bioinformatics tools

Database searches were performed using BLASTP, TBLASTN and PSI-BLAST (http://www.ncbi.nlm.nih.gov/BLAST/). Protein domains were identified using the programs RPS-BLAST (NCBI) and ProfileScan (http://hits.isb-sib.ch/cgi-bin/PFSCAN) searching the Pfam-A, Prosite profiles and Smart databases (NCBI). Nuclear localization signal was detected by using PredictNLS (http://cubic.bioc.columbia.edu/predictNLS/). Amino acid sequence alignments were created using ClustalX 1.8 (http://www-igbmc.u-strasbg.fr/BioInfo/ClustalX) with default parameters and manual adjustments from GeneDoc 2.6.001 (http://www.psc.edu/biomed/genedoc/).

Rapid amplification of cDNA ends (RACE) analyses

5′-RACE and 3′-RACE were performed using a Marathon™ cDNA Amplification Kit (Clontech) with 2 μg of total RNA isolated from adult female flies as template and Advantage® 2 Polymerace Mix in accordance with the manufacturer's recommendations. RACE PCR products were sequenced using a MegaBACE 1000 sequencer.

Sequences of primers used for RACE analyses are available on request. DNA and amino acid sequences derived from the cDNAs were compared and analyzed with the GenBank database.

RT–PCR

Testes and ovaries from adults were dissected in Ringer's solution (6.5 g NaCl, 0.14 g KCl, 0.2 g $NaHCO_3$, 0.12 g $CaCl_2$ and 0.01 g NaH_2PO_4 per liter). Total RNA was isolated from indicated tissues or stages by the use of TRIzol® reagent (Invitrogen), and 5 μg of total RNA were reverse transcribed with SuperScript III RNase H-free reverse transcriptase (RT) (Invitrogen). A random primer pd$(N)_6$ was used for first-strand synthesis. PCR was performed with 2995left (5′-GATGAACGAGAAGTGCGACA-3′, located in exon 5) and 2995right (5′-GATGAACGAGAAGTGCGACA-3′, located in exon 9) primers and with rp49 primers (23) as loading control for 35 cycles at an annealing temperature of 56°C.

Immunostainings and immunofluorescence

The anti-dG9a polyclonal antiserum was raised in rabbits (Eurogentec S.A) against a synthetic peptide containing dG9a residues 1623–1637. The antiserum was affinity purified.

Polytene chromosomes from the salivary glands of third instar larvae were prepared and stained essentially as described in Ref. (24).

Tissues were stained with anti-dG9a (1:25). As secondary antibodies, goat anti-rabbit IgG, conjugated with AlexaFluor 555 (MedProbe, diluted 1:200) were used. Materials were co-stained with DAPI for visualization of DNA. Preparations were analyzed by using a Zeiss Axiophot microscope equipped with a KAPPA DX20C charge-coupled device camera. Staining of larval tissues, ovaries and embryos were performed using standard techniques with anti-dG9a, as described above. Preparations were analyzed by using a ZeissAxioplan2 microscope equipped with a Zeiss AxioCam HRc camera, software: AxioVision3.1. Images were assembled, contrasted and merged electronically by using Photoshop 7.0 (Adobe Systems).

Whole-mount *in situ* hybridization

RNA *in situ* hybridization using digoxigenin-labeled antisense RNA probes was performed as described previously (25,26). A cDNA containing *dG9a* was linearized with

BamHI and used as template to make a 674 bp *dG9a* RNA probe.

Western analysis

Nuclear extract from 0–12 h dechorionated embryos (27) was separated on a SDS–PAGE (8%). Proteins were transferred onto PVDF membrane (Amersham) and probed with an anti-dG9a antibody (1:500) using standard procedures. Secondary antibodies conjugated to HRP (Amersham) were used according to the manufacturer's instructions. Detection of antibody signals was performed with chemiluminescence (Pierce).

Generation of baculovirus, viral transfection and dG9a purification

Amino acids 789–1637 of dG9a was PCR amplified with the primers 2995 SpeIFlag (5′-GACTACAAGGACGACGATG-ACAAGATTTGTCTATGTCAGAAGCCTTCC-3′, FLAG tag sequence underlined) and 2995 KpnI (5′-TGCGGTACCCTA-CGCGTGTCCAATTTTCT-3′) cloned into pFastBac(tm)1 (Invitrogen) as a SpeI/KpnI fragment. Site-directed mutagenesis of flag-dG9a (789–1637 amino acid) was performed using the QuickChange kit (Stratagene) with primers CG2995H1536KBstNIfwd (5′-ATGGAAATGTAACCAGG-TTTTTTAACAAGTC GTGTGAGCCGAATG-3′) and CG2995H1536KBstNIrew (5′-CATTCGG CTCACACGAC-TTGTTAAAAAACCTGGTTACATTTCCAT-3′).

FLAG tagged dG9a in pFastBac^{TM}1 was transformed into DH10Bac (Invitrogen) and bacemid purified according to protocol (Invitrogen). A monolayer of SF9 (*Spodoptera frugiperda*) (9×10^5) was transfected with 1 μg of bacemid using Cellfectin Reagent (Invitrogen) and cells were left for 7 days at 26°C. The supernatant was amplified 2–3 times and recombinant viruses were used for test expression. Cell extracts were checked, 48 h post-transfection, for fusion protein expression using anti-FLAG monoclonal antibody (Sigma). For routine protein expression 10 × 150 mm Petri dishes were infected and the cells kept at 26°C. The cells were harvested 48 h post-infection and washed once with 1× phosphate-buffered saline. For purification of FLAG-dG9A protein, infected cells (1.2×10^8) were resuspended in 4 ml of BC300 [25 mM HEPES (pH 7.6), 300 mM NaCl, 1 mM $MgCl_2$, 0.5 mM EGTA, 0.1 mM EDTA, 10% (v/v) glycerol, 1 mM DTT and protease inhibitors] containing 0.05% (v/v) NP40. The cells were sonicated on ice two times for 15 s at 50% amplitude using a Branson sonifier and centrifuged at 15 000 r.p.m. for 30 min and 100 μl 1:1 slurry of M2 anti-FLAG agarose beads (Sigma) was added to the supernatant followed by incubation for 2 h at 4°C. After washing three times with BC300 [containing 0.05% (v/v) NP40] for 10 min each, and once with BC100 [0.05% (v/v) NP40] the bound protein was eluted with 0.5 mg/ml FLAG peptide BC100 [0.05% (v/v) NP40] for 2 h. The purity of the protein was checked by SDS–PAGE. Eluates were stored at −80°C.

Histone purification and nucleosome assembly

Recombinant *Drosophila* histones were expressed and purified from *Escherichia coli* BL21(DE3)pLys, and reconstituted into octamers as described previously (28). Recombinant histone H3 carrying the mutations K9A, K27A or K9A/K27A were expressed from plasmids kindly provided by D. Reinberg, and histone H4 carrying a K20A mutation was expressed from a plasmid given by T. Jenuwein. Recombinant H4 N-terminal mutant proteins Δ5, Δ10, Δ15, Δ19 were expressed and purified as described previously (29). Native histones were purified from 0–12 h *Drosophila* embryos essentially as described in Ref. (30). Nucleosomes were reconstituted on circular pBS(KS) (Stratagene) by salt dialysis over night from 2 to 0.1 M NaCl (31).

Histone methyltransferase assay

Histone methyltransferase assays were performed as described in Ref. (32). In short, 100 ng of eluted dG9a was mixed with 1 or 2 μg of histone H3, H4, octamer or nucleosomes and S-adenosyl-[methyl-^{3}H]-l-methionine (25 μCi/ml) (Amersham) in a buffer containing 12.5 mM Tris–HCl, pH 8.8, 1 mM DTT, 50 mM NaCl, 50 ng/μl BSA and 2.5 mM $MgCl_2$. The reaction was incubated at 30°C for 1 h and stopped by adding SDS–PAGE loading buffer. The histones were separated by 15% SDS–PAGE, Coomassie stained, amplified and dried. The autoradiograph was developed after 1 and 2 weeks. For experiments with mouse G9a, we used 250 ng of protein and the incubation time was 30 min. Exposure time for autoradiograph was 1 and 2 days.

MALDI-TOF analysis

Methylation reactions were carried out as described above with 0.5 μg of histone H3 or H4 and 250 μM of S-Adenosylmethionine (New England BioLabs). The reaction was stopped by addition of SDS–PAGE loading buffer and the histones were separated by 15% SDS–PAGE. The Coomassie stained bands corresponding to H3 and H4 were excised and subjected to chemical modification to derive free amino groups of lysine residues as described previously (33). H3 and H4 were digested over night with 100 ng of sequencing-grade trypsin (Promega) in a total volume of 40 μl according to manufacturer's protocol. In order to purify the methylated peptides from contaminating salts or acrylamide the peptide solution was passed over a pipette tip containing C18 material (ZipTip, Millipore) and eluted as described previously (32). The MALDI spectra were acquired and analyzed as described previously (34). Reaction mix without enzyme was used for calibration. Quantification was performed as previously described in Ref. (35).

Ecdysone feeding experiments

The feeding experiments were performed essentially as described in Ref. (36).

RESULTS

CG2995 is the *Drosophila* homolog of the mouse G9a HKMTase

We performed a bioinformatics search of the *D. melanogaster* genome with the Su(var)3–9, E(Z) and Trithorax SET domains and found novel genes encoding putative SET proteins. Performing a BLASTP search with the SET domain of one of these proteins, the annotated CG2995 protein,

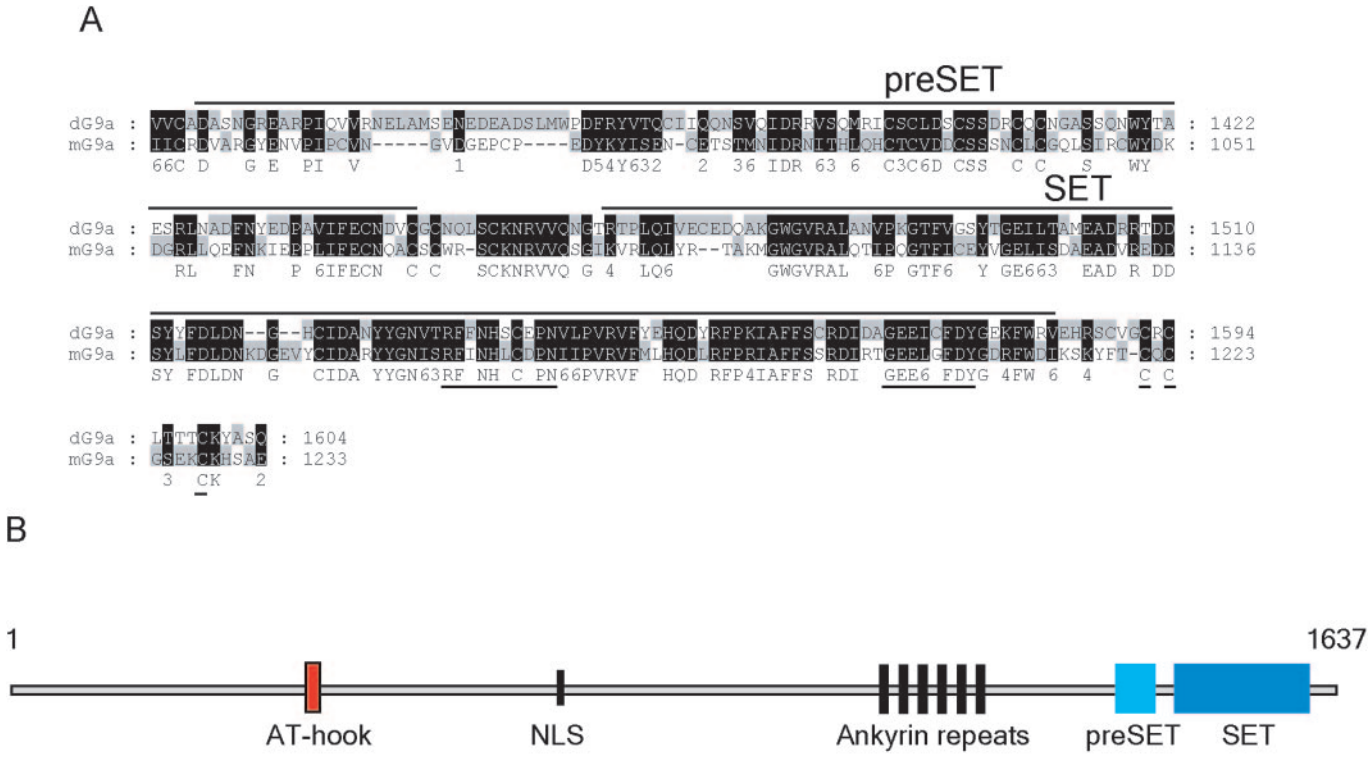

Figure 1. The domain organization is conserved between dG9a and G9a. (**A**) Alignment of SET domains and flanking cysteine-rich regions of mouse and *Drosophila* dG9a protein. The degree of conservation is distinguished at four levels (100, 80 and 60%, and not conserved), where 100% has the darkest shade of grey. The upper and lower case letters in the consensus line indicate 100 and 80% conservation within all groups, respectively. Numbers in the consensus line represent conserved similarity groups as defined by the Blossum 62 scoring table. The conserved R(H)ΦΦNHSC and the FDYG motifs are underlined. (**B**) Domain organization within *Drosophila* protein dG9a. An AT-hook and an ankyrin motif are found in addition to the SET domain.

against the mouse and human database identified it as the *Drosophila* homolog of the G9a protein. This SET domain alone shares 61% identity (76% similarity) with the corresponding domain of the mouse G9a protein (Figure 1A). In comparison, the SET domain of CG2995 shares 45% identity with the SET domain of the Su(var)3–9 protein of *Drosophila*, suggesting that CG2995 is the only homolog of G9a in the *Drosophila* genome. This is emphasized when looking at the pre-SET/SET/post-SET regions, where it is notable that CG2995 is more similar to mouse G9a than to Su(var)3–9 or dSET2. Thus, dSu(var)3–9 versus G9a shows 37% identity, 55% similarity, dSET2 versus G9a displays 36% identity, 50% similarity, and CG2995 versus G9a has 47% identity, 68% similarity. *CG2995* is located as the third gene in region 1A1 on the X chromosome, and a further comparative analysis of the CG2995 protein with the mouse G9a shows that the CG2995 has 33% identity and 49% similarity to the mouse protein (1172–1263 amino acid). The fly protein is longer at the N-terminus but otherwise shares the same module organization as its mouse counterpart. The CG2995 protein contains multiple putative domains in addition to the SET domain, like the adjacent cysteine-rich regions [the pre-SET (also called SAC); (37)], and conserved cysteine residues in the C-terminal region of the SET domain that corresponds to the post-SET domain (Figure 1A), which has shown to be required for enzymatic activity (38). Within the SET domain, a H(R)ΦΦNHSC motif (where Φ indicates a hydrophobic residue) has previously been shown to be an important catalytic site. For SUV39H1 protein, a histidine-to-arginine mutation of the first histidine (His^{320}) in the ^{320}HΦΦNHSC^{326} motif resulted in a 20-fold higher catalytic activity (38). This observation suggests that the H(R)ΦΦNHSC motif is correlated with the HKMTase activity. The CG2995 protein contains a ^{1532}RΦΦNHSC^{1538} motif (Figure 1A, underlined), together with another motif reported to be needed for HKMTase activity, $GE(x)_5Y$, located in the C-terminal end of the SET domain (38; Figure 1A, underlined).

In addition, the CG2995 protein harbors contiguous copies of a 33-amino acid repeat (Figure 1B). This repeat, originally identified in the Notch protein of *Drosophila* and known as the ankyrin repeat, is also found in G9a and in a number of other proteins involved in intracellular protein–protein interactions (39).

An AT-hook also is found in the N-terminus part of the CG2995 protein. The AT-hook is a small DNA-binding protein motif that was first described in the high mobility group non-histone chromosomal protein HMG-I(Y). Since its discovery, this motif has been observed in other DNA-binding proteins from a wide range of organisms. Furthermore, AT-hook motifs are frequently associated with known functional domains seen in chromatin proteins and in DNA-binding proteins (e.g. histone folds, homeodomains and zinc fingers). In general, it appears that the AT-hook motif is an auxiliary protein motif co-operating with other DNA-binding activities and facilitating changes in the structure of the DNA either as a polypeptide on its own [e.g. HMG-I(Y)] (40) or as part of a multidomain protein

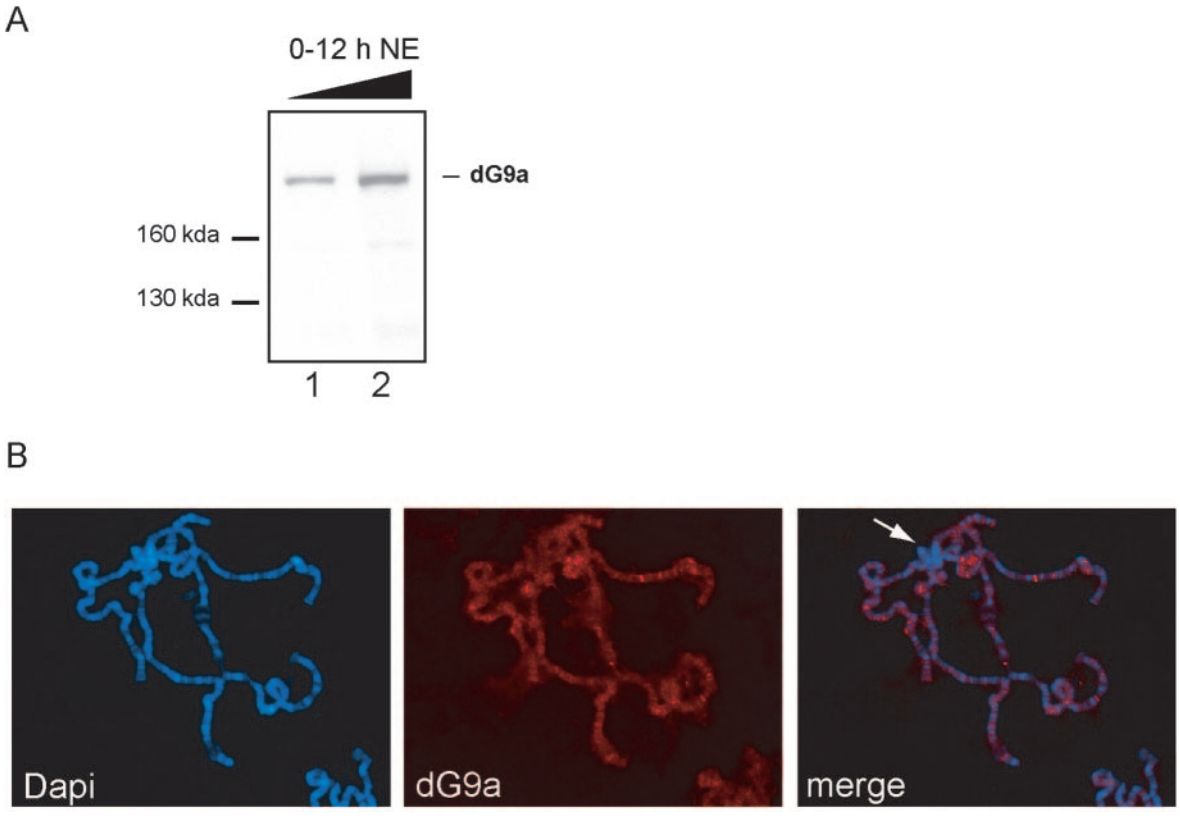

Figure 2. The dG9a protein localizes to distinct chromosome bands. (**A**) Antibodies against dG9a raised in rabbit are specific and recognize a single band of ~180 kDa as predicted on a western blot of *Drosophila* nuclear extract. (**B**) dG9a protein (in red) localizes to chromatin and gives a distinct banding pattern on polytene chromosomes. There is no staining in the chromocenter (arrow), and dG9a localizes predominantly to euchromatic regions. DNA is counterstained with DAPI (in blue).

[e.g. Swi2p in *Saccharomyces cerevisiae* or HRX (ALL-1) in *Homo sapiens*] (41). It is most interesting that this motif seems to be specific to known or predicted chromosomal/DNA-binding proteins, suggesting that it may act as a versatile minor groove tether (41). A nuclear localization signal is found in the N-terminal of the protein. In conclusion, CG2995 has a high level of similarity to mouse G9a and we suggest CG2995 is the *Drosophila* homolog of G9a and will refer to it as dG9a.

Full-length cDNA was cloned by RACE and RT–PCR. This cDNA revealed that the *dG9a* gene consists of 10 exons with a 4911 bp open reading frame (ORF) encoding a protein of 1637 amino acid. The coding region ends by an in-frame stop codon that is followed by a poly(A) signal 1173 downstream, suggesting that it is full-length and consistent with the annotated sequence in FlyBase (http://flybase.bio.indiana.edu/; Figure 1B). Northern analysis also showed that there is only one transcript of expected size (data not shown).

The dG9a protein localizes to euchromatin

Antibodies specific to dG9a were generated by immunization of rabbits with a peptide corresponding to the last 14 amino acids (1623 through 1637 amino acid). This antibody recognized a band of the predicted size of ~180 kDa (Figure 2A). The localization of dG9a protein was investigated by analysis of polytene chromosomes from salivary glands (Figure 2B). The immunostaining showed discrete banding pattern in euchromatic regions with no staining observed in the chromocenter.

Spatiotemporal expression of *dG9a*

To investigate the spatiotemporal expression of *dG9a* we first used semi-quantitative RT–PCR. As shown in Figure 3A, a low but measurable amount of *dG9a* transcript is present in 0–3-h-old embryos. In 3–6-h-old embryos the expression of *dG9a* is barely detectable, indicating that the *dG9a* transcripts seen in 0–3-h-old embryos are of maternal origin. Between 6 and 21 h of embryogenesis the expression of *dG9a* is low but clearly discernible, and about the same level of expression is observed throughout larval development, with a slightly elevated expression during the third larval instar. Then, in 12–46-h-old pupae there is no or very little expression of *dG9a*. In adult flies the expression of *dG9a* is restricted to the gonads in both sexes (Figure 3A, last four lanes). However, we cannot rule out the possibility that *dG9a* is expressed in one or more tissues of the gonadectomized flies, but at a level too low to be detected by the RT–PCR settings used here.

Next, in order to study the spatiotemporal expression of dG9a in more detail, we stained ovaries and embryos with the dG9a antibody. The immunostainings revealed that dG9a is expressed in all cells of the ovary, including the germarium (Figure 3C) where especially the nurse cells,

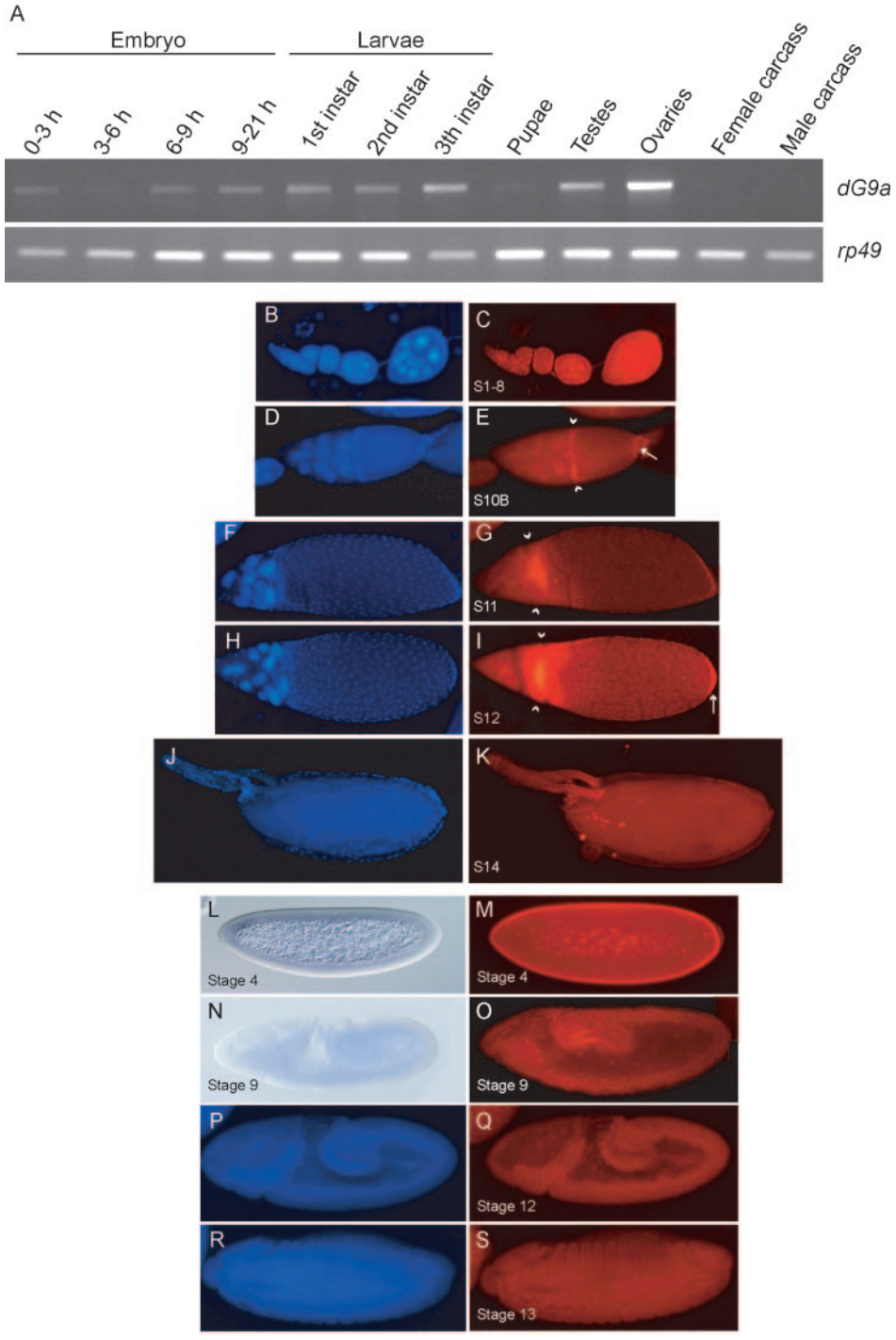

Figure 3. Spatiotemporal expression of dG9a. (**A**) Developmental RT–PCR shows that *dG9a* is maternally deposited in the egg, and that there is moderate expression during the larval development. dG9a is present in all developmental stages investigated. (B–K) dG9a is present from the very start of oogenesis through the end of oogenesis in wild-type ovarioles. Anterior is to the left, posterior to the right. dG9a in red (right column) and the nuclei is counter stained with DAPI in blue (left column). (**B** and **C**) The early stages of oogenesis development. The dG9a protein is present from the very start. (**D** and **E**) Stage 10B ovaries. dG9a localizes to nuclei in both nurse and follicle cells. An accumulation of protein is observed in the region where the anterior polar cells and the centripetal follicle cells are located, arrowheads and in the posterior follicle cells, arrow. (**F** and **G**) Stage 11. Shortly after centripetal migration (stage 10B), the nurse cells rapidly transfer their contents into the oocyte (stage 11) then begin to degenerate and undergo apoptosis (stages 12–14). (**H** and **I**) Stage 12. Dumping complete, no or very little dG9a is detectable in the degenerating nurse cell nuclei, but is still present in the follicle cells. Notice the accumulation of dG9a protein in the extreme posterior part of the egg, arrowheads, where the posterior polar cells located. (**J** and **K**) Stage 14. The egg is fully developed and dG9a protein is maternally deposited. (L–S) Lateral views of wild-type embryos hybridized with digoxigenin-labeled RNA probes (L and N with Nomarski optics) or with a dG9a antibody (**M, O, Q** and **S**). Anterior is to the left and dorsal is up. The nuclei are counter stained with DAPI in blue. (**L** and **M**) Embryo at syncytial blastoderm stage (stage 4, ~1.5–2.5 h). dG9a is localized to the nuclei. In early embryos the message and the protein are ubiquitously distributed due to its maternal contribution. (**N** and **O**) Embryo during germband extension (stage 9). (**P** and **Q**) Stage 12. In late-stage embryos, expression is strongest in the CNS and the neuroectoderm. (**K** and **S**) Stage 13. Surface view of embryo at the completion of germband shortening.

which undergo a dramatic endoreplication, stain heavily. It also clearly shows that dG9a is localized to the nucleus. In stage 10B egg chambers it appears that dG9a is markedly upregulated in what appears to be the centripetal follicle cells (Figure 3E, arrowheads). At this stage, a moderate upregulation is also discernible in the posterior follicle cells (arrow). During stage 11 nurse start dumping their content into the oocyte, which is revealed by an accumulation of dG9a at the border between the growing oocyte and the degenerating nurse cells (Figure 3G). At this stage an increased expression of dG9a is also found in the posterior follicle cells (Figure 3G, arrow head). In stage 12 the amount of dG9a has increased considerably and has started to move into the oocyte. An accumulation in the posterior follicle cells is now prominent (Figure 3I, arrow). At stage 14, dG9a appears to be evenly distributed in the mature oocyte (Figure 3K).

In blastoderm embryos (stage 4, ~1.5–2.5 h) *dG9a* transcript as well as protein are present in the syncytial nuclei (Figure 3L and M). During stages 9 and 12, dG9a expression appears to be more abundant in the central nervous system (CNS) and the neuroectoderm (Figure 3N, O and Q). Figure 3S shows a surface view of embryo at the completion of germband shortening, with all cells evenly stained.

Expression and purification of recombinant histone methyltransferase dG9a

In order to investigate the enzymatic properties of dG9a we expressed a FLAG tagged N-terminal fragment (789–1637 amino acid) using a baculovirus expression system. The purified dG9a was soluble and had the expected molecular size of 95 kDa (Figure 4A). To confirm that dG9a has HKMTase activity we incubated it in presence of H^3-S-adenosylmethionine (SAM) and different substrates (Figure 4B). dG9a methylates H3 and H4 present as free histones but had no detectable activity on nucleosomal arrays. In contrast to the recombinant dG9a, mouse G9a only methylates H3 even when other histones are present (Figure 4C). In order to exclude the possibility that the unexpected H4 HMT activity is due to a contaminating activity co-purifying with the recombinant dG9a we expressed the enzyme carrying a point mutation within the SET domain (H1536K) that dramatically impairs its catalytic activity. The mutated enzyme was not able to methylate either H3 or H4 indicating that both methylations are a result of dG9a activity (Figure 4D). In order to determine the substrate specificity we performed a quantitative MALDI-TOF analysis of H3 molecules methylated by dG9a. Similarly to the activity of the mouse ortholog (42), dG9a methylates exclusively K9 and K27 with K9 being the preferred substrate in wild-type (wt) H3. As shown for mG9a (43) dG9a is able to add up to three methyl groups to H3 (Figure 4H). This finding is confirmed by using H3 molecules carrying a lysine to alanine replacement at position 9 and 27 or both (Figure 4E). We observe decreased methylation efficiency on H3 K9A and H3 K27A compared to wt H3. In a filter binding assay we observed a 70% reduction when K9 was mutated and a 50% reduction when K27 was mutated. When both H3 lysine residues were mutated (K9A and K27A) we observe a lower activity (efficiency of 27%) indicating that in absence of K9 and K27 dG9a is also able to methylate other lysines. Mouse G9a also showed a decreased activity (27%) towards the double mutant (K9A/K27A) (Figure 4F). When we use highly active mG9a (43), it methylates wt H3 and the H3 molecules carrying a single mutation on K9 or K27 with a similar efficiency. However, as we use relatively long reaction times we can not exclude the possibility that K9 is methylated faster than K27, which explains the larger differences observed in previous publications (16,44).

Interestingly dG9a was also able to methylate histone H4 (Figure 4B). This is in marked contrast to the mouse G9a where we do not observe such an activity (Figure 4C) (42). The only lysine residue of H4 shown to be methylated *in vivo* is K20 and the first HKMTase identified with this activity was hPR-Set7/dSET8 (45,46). Other HKMTases in *Drosophila* shown to methylate H4 lysine 20 are Ash1 and Suv4–20 (47,48). Ash1 is in addition able to methylate lysine 4 and 9 in histone H3 (47). From these experiments we concluded that dG9a also is a multi-catalytic histone methyltransferase with specificity for lysine 9 and 27 on H3 and possibly lysine 20 on histone H4. However, when we incubated dG9a with H4 carrying a mutation of lysine 20 to alanine we observed no reduction of activity (Figure 4G). To further investigate the specificity, we tested whether dG9a was able to methylate H4 molecules carrying different N-terminal deletions (29). We observed that dG9a could methylate the H4 N-terminus when the first five amino acids were deleted, excluding K5 as a possible substrate. However, the activity was lost when we used the H4 Δ10 mutant (Figure 4G). This suggests that the substrate is K8, but considering that the minimal substrate specificity for mG9a surrounding K9 contains seven amino acids (TARKSTG) (49) we cannot exclude that another downstream lysine can serve as a substrate. MALDI-TOF analysis of H4 methylated by dG9a, showed that only the peptide containing amino acids 4–17 was methylated *in vitro* (Figure 4H). We conclude from these experiments that dG9a can methylate lysine 8, 12 or 16 of H4 *in vitro*. It remains to be seen to what level these lysines are methylated *in vivo* and what the function of this methylation is.

dG9a is required for normal development

To investigate the *in vivo* function of dG9a, transgenic flies with an inverted-repeat *UAS-dG9a.IR* construct were crossed to different GAL4-driver lines (22). The vector used for making the inverted repeats has an independent UAS-GFP marker so that a tissue exposed to RNAi will simultaneously show GFP expression [pUds-GFP; (21)] as an internal control to RNAi expression. In addition, down regulation of *dG9a* was confirmed by RT–PCR (Figure 5A).

Using the ubiquitously expressed *da-GAL4* driver with the *UAS-dG9a*.IR flies, the progeny developed normally until the end of the third larval instar. However, these RNAi larvae did not form their puparium and crawling larvae were found after 7–8 days (Figure 5B). The majority of these larvae developed melanotic tumors, either one or two larger ones or several smaller. The larvae finally stopped moving, and in the few cases where 'pseudo-prepupae' were formed,

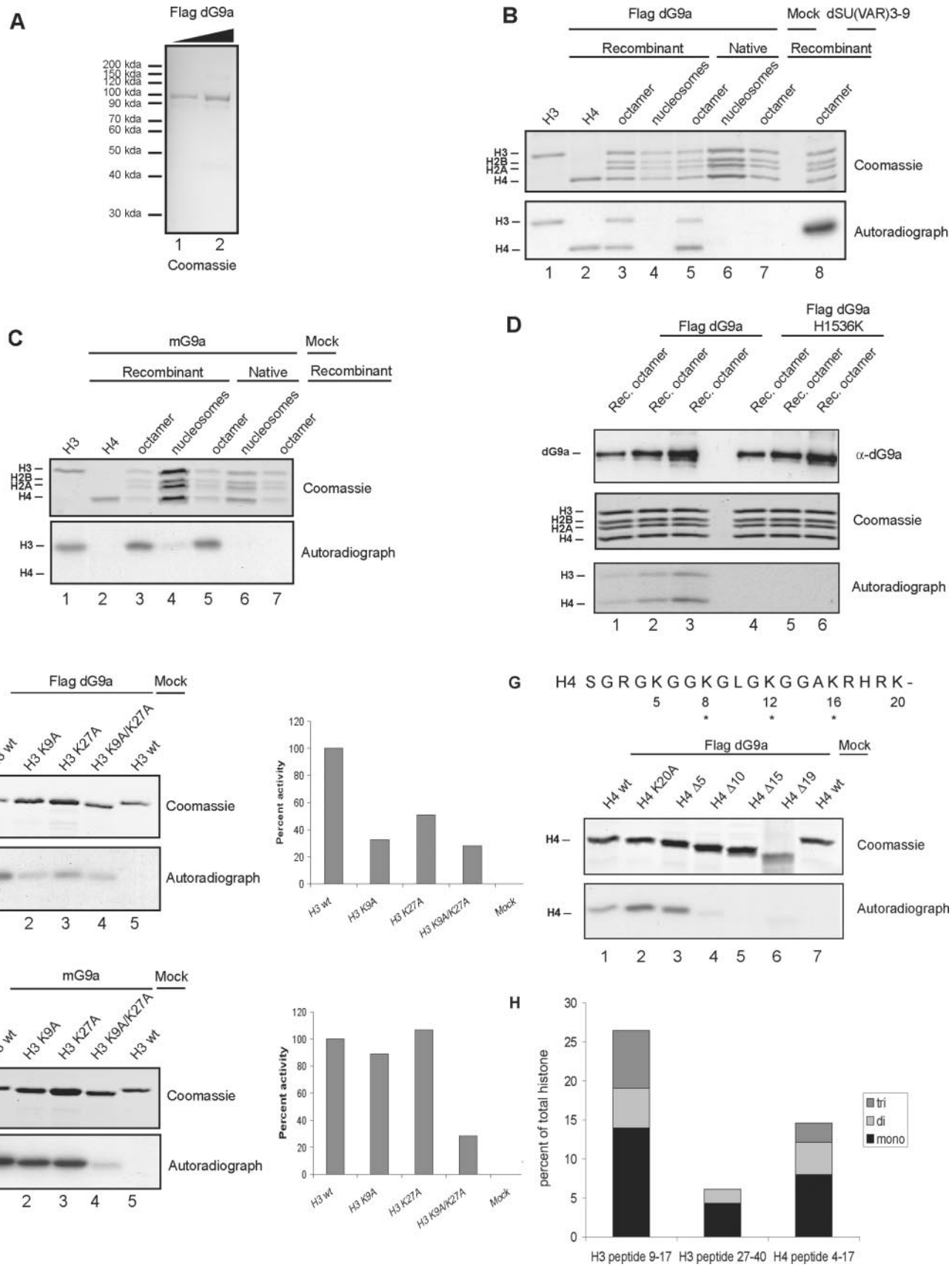
A
Flag dG9a
200 kda
150 kda
120 kda
100 kda
90 kda
70 kda
60 kda
50 kda
40 kda
30 kda
1 2
Coomassie
B
Flag dG9a
Mock dSU(VAR)3-9
Recombinant
Native
Recombinant
H3
H4
octamer
nucleosomes
octamer
nucleosomes
octamer
octamer
H3
H2B
H2A
H4
Coomassie
Autoradiograph
1 2 3 4 5 6 7 8
C
mG9a
Mock
Recombinant
Native
Recombinant
H3
H4
octamer
nucleosomes
octamer
nucleosomes
octamer
Coomassie
Autoradiograph
1 2 3 4 5 6 7
D
Flag dG9a
Flag dG9a H1536K
Rec. octamer
dG9a
α-dG9a
Coomassie
Autoradiograph
1 2 3 4 5 6
E
Flag dG9a
Mock
H3 wt
H3 K9A
H3 K27A
H3 K9A/K27A
H3 wt
Coomassie
Autoradiograph
1 2 3 4 5
Percent activity
H3 wt
H3 K9A
H3 K27A
H3 K9A/K27A
Mock
F
mG9a
Mock
H3 wt
H3 K9A
H3 K27A
H3 K9A/K27A
H3 wt
Coomassie
Autoradiograph
1 2 3 4 5
Percent activity
G
H4 S G R G K G G K G L G K G G A K R H R K -
5 8 12 16 20
Flag dG9a
Mock
H4 wt
H4 K20A
H4 Δ5
H4 Δ10
H4 Δ15
H4 Δ19
H4 wt
Coomassie
Autoradiograph
1 2 3 4 5 6 7
H
percent of total histone
tri
di
mono
H3 peptide 9-17
H3 peptide 27-40
H4 peptide 4-17

these maintained the elongated larval form and failed to evert the anterior spiracles; there was only slight melanization of these 'pseudo-prepupae' (Figure 5C).

The defects in puparium formation seen in *dG9a* RNAi animals could result from either a decrease in the ecdysone titer or a decrease in the ability of the ecdysone signal to be transduced. To distinguish between these possibilities we examined the effects of feeding ecdysone to *dG9a* RNAi larvae. This method has been shown to effectively rescue phenotypes associated with ecdysone-deficient mutations (36). Mid- and late-third instar larvae were transferred to food either with or without 20-hydroxyecdysone (20E) for 6–8 h and scored on a 12-h basis. Feeding 20E to *dG9a* RNAi larvae did not rescue them to puparium formation. Therefore, we conclude that ecdysone is not limiting in the *da-GAL4/UAS-dG9a.IR* animals and that *dG9a* functions downstream of ecdysone biosynthesis and release.

When the ubiquitously expressed, but weaker, *Act5C-GAL4* driver was used, development of progeny of genotype *Act5C-GAL4/UAS-dG9a.IR* proceeded up to and through puparium formation (data not shown). However, most of the pupal cases were only lightly tanned and no flies eclosed from these cases. Upon dissection, dead and partially differentiated pharates with no eye pigmentation or legs were found (data not shown). Development appeared to have proceeded further in the posterior part of fly. Of all pupae formed ($N = 133$), ~17% developed normally, and the eclosed flies were without exception females.

As immunostaining indicated a role for dG9a in neuroectoderm and CNS, a driver which expresses GAL4 in brain and throughout CNS, but not in discs, of third instar larvae, P{GawB}c698a, was used. The phenotypes observed were similar to those observed with the *Act5C-GAL4* driver. Here, however, most of the pupae were partly more melanized (Figure 5D), without differentiation proceeding any further than that described for the *Act5C-GAL4* driver (Figure 5E). A small portion (~5%) of the pupae actually developed normally but of these almost all failed to escape from the pupal case. The very few that succeeded were all normal females and lived for at least 2 weeks.

The results described above strongly suggest a defect in ecdysone responses at puparium formation, similar to those reported earlier for mutants in the ecdysone pathway (50). Also, using RNAi very similar results were obtained with the H3–K36 HKMTase *dSet2* gene (M. Stabell, unpublished data).

Ecdysone controls wing morphogenesis and cell adhesion by regulating integrin expression during metamorphosis (51). Therefore, to test further the possible involvement of dG9a in the ecdysone regulation hierarchy, we triggered *dG9a* RNAi in the wing disc by the *ap-GAL4* driver. This resulted in slightly held-out/up wings with an anterior–posterior compression (Figure 5F), and occasionally in blister formation (Figure 5G). We next generated flies of genotype *ap-GAL4,UAS-dG9a.IR/EcR*^{M554fs}. *EcR*^{M554fs} is a loss of function mutation where only half the amount of the ecdysone receptor is present in mutant flies. As shown in Figure 5I, these animals show a wing phenotype of a more extreme character, with both wings having a blister and being clearly smaller than normal, most likely because the wings never completely unfold. This phenotype has 100% penetrance. Taken together, these results support the notion that dG9a functions in ecdysone signaling pathways during development.

DISCUSSION

dG9a is a euchromatic histone methyltransferase

In this study we show that CG2995 is the *Drosophila* homolog of the HKMTase G9a, and that it specifically mono-, di- and trimethylates H3–K9, H3–K27 and K8, 12 or 16 in H4. This methylation pattern is mainly correlated with silencing (11) suggesting that dG9a is involved in transcriptional repression. Further, we showed that dG9a methylates free histones but has no detectable activity on nucleosomal arrays. As revealed by the staining of polytene chromosomes, the centromeric region, where Su(var)3–9 predominantly stains (52), is devoid of dG9a. We therefore conclude that dG9a is a euchromatic histone methyltransferase that acts on loosely packed DNA and that methylation by dG9a may occur on pre-assembled histones.

Figure 4. Characterization of recombinant dG9a. (**A**) Eluted FLAG tagged dG9a (789–1637 amino acid) was separated on a 12% SDS–PAGE and stained with Coomassie blue G250. (**B**) *In vitro* methylation reactions using dG9a (lanes 1–6), no enzyme (lane 7) and dSu(var)3–9 (lane 8). In the reaction we used 1 μg of different histones: recombinant histone H3 (lane 1), recombinant histone H4 (lane 2), recombinant (lane 3) and native histone octamer (lane 5) and recombinant and native nucleosomes (lanes 4 and 6) reconstituted on circular pBS(KS) from equimolar amounts of histones. The upper panel shows Coomassie stained gel and the lower panel the autoradiograph. (**C**) Activity of recombinant mouse G9a expressed in baculovirus infected cells (a kind gift from S. Pradhan). HKMTase activity on 1 μg of different histone substrates: recombinant histone H3 (lane 1), recombinant histone H4 (lane 2), recombinant and native histone octamers (lanes 3 and 5) and recombinant and native nucleosomes (lanes 4 and 6). Mock control (lane 7) is incubation of recombinant octamer without enzyme. The Coomassie gel is shown at the top and the corresponding autoradiograph at the bottom. (**D**) FLAG dG9a wild type versus H1536K mutation of the conserved region of the SET domain. The upper panels shows a western blot of the two proteins. Recombinant octamer (2 μg) was used as substrate for 25. 50 and 100 ng of wt (lanes 1–3) and H1536K mutant (lanes 4–6). The corresponding autoradiograph is shown in the lower panel. (**E**) *In vitro* methylation of 2 μg of recombinant H3 (lane 1), H3 mutated at lysine 9 (lane 2), H3 mutated at lysine 27 (lane 3) or both (lane 4) using dG9a and a mock purification. Coomassie stained H3 is shown in the upper panel and a corresponding autoradiography in lower panel. A corresponding filter binding assay is shown to the right. The *y*-axis displays the percent radioactivity incorporated on 2 μg of histone H3 and H3 mutants K9A, K27A and K9/K27A with radioactivity incorporated on wt H3 set to 100% and the background is subtracted. (**F**) HKMTase activity of mG9a on histone H3 molecules and H3 K9A, H3 K27A and the double mutant K9A/K27A. A gel of Coomassie stained histones and the corresponding autoradiography is shown. On the right, a filter binding assay showing percent radioactivity incorporated on 2 μg of histone H3 and H3 mutants K9A, K27A and K9/K27A. The *y*-axis displays the percent radioactivity incorporated with activity on wt H3 set to 100% and the background is subtracted (**G**) Amino acid sequence of the H4 N-terminus is shown at the top. Asterisks indicate possible substrates for dG9a *in vitro*. Methylation of 2 μg of recombinant H4 (lane 1), H4 K20A (lane 2), H4Δ5 (lane 3), H4Δ10 (lane 4), H4Δ15 (lane 5) and globular H4 (lane 6). Mock control (lane 7) is incubation of wt H4 without enzyme. (**H**) Quantitative MALDI-TOF analysis of 500 ng of H3 and H4 methylated by 100 ng of dG9a. Peptides spanning amino acids 9–17 and 27–40 of H3 and 4–17 of H4 is represented by graphs. No signals were observed in other peptides. Mono-, di- and trimethylation are shown as percent of total H3 or H4. This figure is representative for at least three different methyltranferase assays.

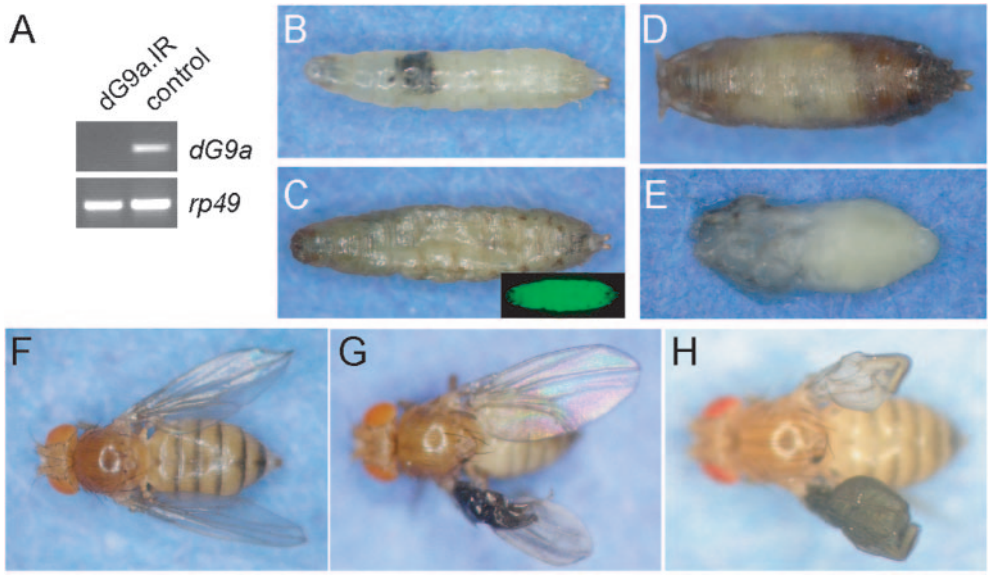

Figure 5. Knock down of *dG9a* give phenotypic effects. RNAi experiments show that dG9a is important for development. (**A**) RT–PCR shows that *dG9a* is down regulated by RNAi; *rp49* is used as loading control. (**B** and **C**) Using a ubiquitously expressed driver, *da-GAL4*, to induce the IR construct shows that dG9a is required for proper transition from larva to pupa. Penetrance is 100%. In (B) the larva is 6 days, in (C) 8 days. The IR construct is tagged with an independent UAS-GFP, which can be used as control (insert). Melanotic tumors are frequently observed in these larvae. (**D** and **E**) Using a larval *CNS-GAL4* (BL 3739) driver the progeny makes it up to and through pupariation (**F**), but fails to hatch. Differentiation seems more complete in posterior part of the animal (**G**). A similar phenotype is observed when using *Act5C-GAL4* as driver. Remarkably, in both cases, the escapers observed to hatch (~10%) are females. (**H** and **I**) When using the *ap-GAL4* driver defects in the wings are observed. This phenotype is highly pleiotropic, with one or both wings affected. Among the phenotypes are narrow wings held in a Dichaeate-like fashion, wings standing straight up and blistered wings. Progeny with no apparent defects are also observed. (**J**) Progeny of genotype *ap-GAL4,UAS-dG9a.IR*/EcR^{M544fs} show a wing phenotype of severe character and 100% penetrance.

dG9a is expressed throughout development

Immunostaining revealed that the dG9a protein is found throughout oogenesis, embryogenesis, and larval development. During these stages, large cells (like nurse cells and salivary gland cells) are metabolically very active, and having multiple copies of genes (polyteny) permits a high level of gene expression; that is, abundant transcription and translation to produce the gene products. (53). In adult flies the *dG9a* transcript and protein are solely found in the gonads, where cells are undergoing extensive endo- and mitotic replication. One can assume that is important that certain genes are kept silent in these cells, and one possible function of dG9a could be to maintain repression of a subset of genes in cells that otherwise have a high gene expression level.

In the RNAi knock down studies, no lethality was observed during embryogenesis, but this can be ascribed to the fact that the RNAi construct was made using a pUAST based vector that is defect in the germline during oogenesis (22). Conditional knock down of dG9a in the female germline was therefore not possible in this study, but should be subject for future investigation. An interesting observation is that the escapers from the RNAi studies are exclusively females. This result suggests that dG9a may have different roles in males versus females. It is possible that conditional depletion of dG9a in transgenic flies may affect the expression of genes that are required for chromatin stability, chromosome segregation and proper histone modifications resulting in a preferential lethality in male flies. This has recently been reported for *Su(var)205* (also called *HP1*) (54), and *bonus* (*bon*), encoding a homolog of the vertebrate TIF1 transcriptional cofactors and required for male viability (55). Interestingly, bon is associated with genes that are implicated in the ecdysone pathway.

dG9a is involved in ecdysone mediated signaling

Next, we provide evidence that dG9a is required for important transitions during *Drosophila* development. Our results suggest a role for dG9a in regulation of genes, especially during the onset of metamorphosis, and wing development, processes tightly correlated to ecdysone responsive signaling (56). Additional evidence for dG9a being involved in the ecdysone hierarchy is the formation of melanotic tumors in the larvae that do not form their puparium. Several chromatin-modifying or chromatin-associated complexes (57) as well as ecdysone have been implicated in hemocyte development and melanotic tumor formation (58,59). Furthermore, our genetic studies revealed that the EcR^{M544fs} is able to dominantly affect the wing phenotype in *ap-GAL4,UAS-dG9a.IR*/EcR^{M554fs} flies. Genetic interactions between mutant alleles of different genes are indicative of these genes belonging to the same functional pathway. Thus, the genetic studies support the results from the RNAi experiments, and together provide strong evidence of dG9a being involved in the ecdysone signaling hierarchy. As the RNAi mutants are not rescued by hormone feeding, dG9a must exert its effect downstream of ecdysone biosynthesis and metabolism. One possible scenario is that dG9a acts as a co-regulator for the ecdysone receptor mediating downstream gene regulation as a response to ecdysone pulses. A similar scenario has been reported for mammalian G9a, where a reduction of endogenous G9a reduced hormonal activation of an endogenous target gene by the androgen receptor (60).

The genetic interaction between EcR^{M554fs} and *ap-GAL4,UAS-dG9a.IR* on wing development may suggest a molecular interaction between the EcR receptor and dG9a. Activation and repression of transcription involve the recruitment of many co-regulator (co-repressor or co-activator) proteins to the regulated gene promoter by sequence-specific DNA binding transcription factors. As dG9a contains an AT-hook, it could tether the ecdysone receptor to the DNA, or, more plausible, the DNA binding activity of EcR by could bring dG9a to the promoter. Two models could explain the EcR-dG9a relationship observed:

(i) dG9a act as a co-repressor of the early puffs according to the Ashburner model for the hormonal control of polytene chromosome puffing (61). Briefly, this model proposed that ecdysone, bound to its specific receptor, directly induces the expression of a small set of early regulatory genes. The protein products of these genes, in turn, repress their own expression and induce a much larger set of late target genes. dG9a could be involved in this repression.
(ii) dG9a act as a co-activator coupled to the transcription apparatus during activation of ecdysone regulated genes.

Vakoc and co-workers (62) reported recently that H3–K9 methylation was found at high levels in the transcribed region of four genes while they were transcribed. This observation is rather remarkable in that it implies a coupling of the traditionally accounted H3–K9 silencing mark to active transcription. Therefore, the possibility that dG9a plays a role in maintaining transcription should be further investigated. In addition, there are observations that murine G9a acts both as a co-repressor (63–65), and a co-activator (60), depending on promoter context and/or regulatory environment, along with the observation that the zinc finger protein wiz links G9a/GLP histone methyltransferases to the co-repressor molecule CtBP (66). Furthermore, NSD1, which methylates both H3–K36 and H4–K20 *in vitro* (67), acts as a co-activator and a co-repressor for NRs (37).

As a complement to the RNAi approach, we have tried to generate null mutants (deletions) by re-mobilization of the P-element inserted in the 5′-untranslated region (5′-UTR) of *dG9a* in the $dG9a^{13414}$ stock. Whereas several independent lines with precise excision of the P-element were obtained we failed to find any imprecise excision (deletion) events (M. Stabell, unpublished data). During the course of the preparation of this manuscript, Mis *et al*. (68) also identified CG2995 as being the *Drosophila* homolog of mammalian G9a. This group also reported unsuccessful mobilization of the P-element, and suggested that this may be due to a defective P-element. Instead, they investigated the $dG9a^{13414}$/$dG9a^{13414}$ mutant and report only a minor phenotype without characterizing the nature of the mutant. On the other hand, they showed that this $dG9a^{13414}$ mutant suppresses position effect variegation (PEV) and that it interacts genetically with Su(var)3–9, suggesting that the two proteins have an overlapping role in heterochromatic gene silencing and may be members of protein complexes involved gene silencing. In contrast to Mis *et al*. (68) who concluded that dG9a is a H3–K9 HKMTase, we provide evidence that dG9a (i) methylates H4 as well as H3, (ii) is able to add three methyl groups, (iii) methylates K9 and K27 on histone H3 with a preference for K9 and (iv) has a specificity towards K8, K12 or K16 on the H4 N-terminus. In polytene chromosomes dG9a is excluded from the chromocenter (Figure 3), indicating a euchromatic role for dG9a. But as the majority of full-length GFP-mG9a fusion proteins has been found in pericentric heterochromatin (16), we cannot rule out a conceivable function for dG9a during facultative heterochromatinization in other tissues and/or stages of development.

ACKNOWLEDGEMENTS

We would like to thank Sriharsa Pradhan for providing the mouse G9a baculoviral protein, Danny Reinberg for H3 mutant plasmids, Thomas Jenuwein for the H4 K20A plasmid, Cedric R. Clapier and Peter Becker for the H4 N-terminal deletion proteins, Daisy Schwarzlose for providing SF9 cells, Anette Preiss for the pHIBS and pUds-GFP vectors, and Ann Mari Voie at the EMBL injection service for the transgenic lines. This study was supported by a grant from the Norwegian Research Council to R.B.A. and A.L., from the Swedish Research Council to J.L., and from the Deutsche Forsghungsgemeinschaft (IM23/4-3) to A.I. Funding to pay the Open Access publication charges for this article was provided by Norwegian Research Council.

Conflict of interest statement. None declared.

REFERENCES

1. Jenuwein,T. and Allis,C.D. (2001) Translating the histone code. *Science*, **293**, 1074–1080.
2. Strahl,B.D. and Allis,C.D. (2000) The language of covalent histone modifications. *Nature*, **403**, 41–45.
3. Chuikov,S., Kurash,J.K., Wilson,J.R., Xiao,B., Justin,N., Ivanov,G.S., McKinney,K., Tempst,P., Prives,C., Gamblin,S.J. *et al*. (2004) Regulation of p53 activity through lysine methylation. *Nature*, **432**, 353–360.
4. Fischle,W., Wang,Y. and Allis,C.D. (2003) Histone and chromatin cross-talk. *Curr. Opin. Cell Biol*., **15**, 172–183.
5. Lachner,M., O'Sullivan,R.J. and Jenuwein,T. (2003) An epigenetic road map for histone lysine methylation. *J. Cell Sci*., **116**, 2117–2124.
6. Ng,H.H., Feng,Q., Wang,H., Erdjument-Bromage,H., Tempst,P., Zhang,Y. and Struhl,K. (2002) Lysine methylation within the globular domain of histone H3 by Dot1 is important for telomeric silencing and Sir protein association. *Genes Dev*., **16**, 1518–1527.
7. Jenuwein,T., Laible,G., Dorn,R. and Reuter,G. (1998) SET domain proteins modulate chromatin domains in eu- and heterochromatin. *Cell Mol. Life Sci*., **54**, 80–93.
8. Zhang,X., Yang,Z., Khan,S.I., Horton,J.R., Tamaru,H., Selker,E.U. and Cheng,X. (2003) Structural basis for the product specificity of histone lysine methyltransferases. *Mol. Cell*, **12**, 177–185.
9. Cao,R. and Zhang,Y. (2004) SUZ12 is required for both the histone methyltransferase activity and the silencing function of the EED–EZH2 complex. *Mol. Cell*, **15**, 57–67.
10. Wang,H., An,W., Cao,R., Xia,L., Erdjument-Bromage,H., Chatton,B., Tempst,P., Roeder,R.G. and Zhang,Y. (2003) mAM facilitates conversion by ESET of dimethyl to trimethyl lysine 9 of histone H3 to cause transcriptional repression. *Mol. Cell*, **12**, 475–487.
11. Martin,C. and Zhang,Y. (2005) The diverse functions of histone lysine methylation. *Nat. Rev. Mol. Cell. Biol*., **6**, 838–849.
12. Aagaard,L., Laible,G., Selenko,P., Schmid,M., Dorn,R., Schotta,G., Kuhfittig,S., Wolf,A., Lebersorger,A., Singh,P.B. *et al*. (1999) Functional mammalian homologues of the *Drosophila* PEV-modifier Su(var)3–9 encode centromere-associated proteins which complex with the heterochromatin component M31. *EMBO J*., **18**, 1923–1938.

13. Stewart,M.D., Li,J. and Wong,J. (2005) Relationship between histone H3 lysine 9 methylation, transcription repression, and heterochromatin protein 1 recruitment. *Mol. Cell. Biol.*, **25**, 2525–2538.
14. Peters,A.H., Kubicek,S., Mechtler,K., O'Sullivan,R.J., Derijck,A.A., Perez-Burgos,L., Kohlmaier,A., Opravil,S., Tachibana,M., Shinkai,Y. *et al.* (2003) Partitioning and plasticity of repressive histone methylation states in mammalian chromatin. *Mol. Cell*, **12**, 1577–1589.
15. Rice,J.C., Briggs,S.D., Ueberheide,B., Barber,C.M., Shabanowitz,J., Hunt,D.F., Shinkai,Y. and Allis,C.D. (2003) Histone methyltransferases direct different degrees of methylation to define distinct chromatin domains. *Mol. Cell*, **12**, 1591–1598.
16. Esteve,P.O., Patnaik,D., Chin,H.G., Benner,J., Teitell,M.A. and Pradhan,S. (2005) Functional analysis of the N- and C-terminus of mammalian G9a histone H3 methyltransferase. *Nucleic Acids Res.*, **33**, 3211–3223.
17. Tachibana,M., Sugimoto,K., Nozaki,M., Ueda,J., Ohta,T., Ohki,M., Fukuda,M., Takeda,N., Niida,H., Kato,H. *et al.* (2002) G9a histone methyltransferase plays a dominant role in euchromatic histone H3 lysine 9 methylation and is essential for early embryogenesis. *Genes Dev.*, **16**, 1779–1791.
18. Schotta,G., Ebert,A., Krauss,V., Fischer,A., Hoffmann,J., Rea,S., Jenuwein,T., Dorn,R. and Reuter,G. (2002) Central role of *Drosophila* SU(VAR)3–9 in histone H3-K9 methylation and heterochromatic gene silencing. *EMBO J.*, **21**, 1121–1131.
19. Mermoud,J.E., Popova,B., Peters,A.H., Jenuwein,T. and Brockdorff,N. (2002) Histone H3 lysine 9 methylation occurs rapidly at the onset of random X chromosome inactivation. *Curr. Biol.*, **12**, 247–251.
20. Litt,M.D., Simpson,M., Gaszner,M., Allis,C.D. and Felsenfeld,G. (2001) Correlation between histone lysine methylation and developmental changes at the chicken beta-globin locus. *Science*, **293**, 2453–2455.
21. Nagel,A.C., Maier,D. and Preiss,A. (2002) Green fluorescent protein as a convenient and versatile marker for studies on functional genomics in *Drosophila*. *Dev. Genes Evol.*, **212**, 93–98.
22. Brand,A.H. and Perrimon,N. (1993) Targeted gene expression as a means of altering cell fates and generating dominant phenotypes. *Development*, **118**, 401–415.
23. McGuire,S.E., Le,P.T., Osborn,A.J., Matsumoto,K. and Davis,R.L. (2003) Spatiotemporal rescue of memory dysfunction in *Drosophila*. *Science*, **302**, 1765–1768.
24. Larsson,J., Chen,J.D., Rasheva,V., Rasmuson-Lestander,A. and Pirrotta,V. (2001) Painting of fourth, a chromosome-specific protein in *Drosophila*. *Proc. Natl Acad. Sci. USA*, **98**, 6273–6278.
25. Jiang,J., Hoey,T. and Levine,M. (1991) Autoregulation of a segmentation gene in *Drosophila*: combinatorial interaction of the even-skipped homeo box protein with a distal enhancer element. *Genes Dev.*, **5**, 265–277.
26. Tautz,D. and Pfeifle,C. (1989) A non-radioactive in situ hybridization method for the localization of specific RNAs in *Drosophila* embryos reveals translational control of the segmentation gene hunchback. *Chromosoma*, **98**, 81–85.
27. Sandaltzopoulos,R., Mitchelmore,C., Bonte,E., Wall,G. and Becker,P.B. (1995) Dual regulation of the *Drosophila* hsp26 promoter *in vitro*. *Nucleic Acids Res.*, **23**, 2479–2487.
28. Luger,K., Mader,A.W., Richmond,R.K., Sargent,D.F. and Richmond,T.J. (1997) Crystal structure of the nucleosome core particle at 2.8 A resolution. *Nature*, **389**, 251–260.
29. Clapier,C.R., Nightingale,K.P. and Becker,P.B. (2002) A critical epitope for substrate recognition by the nucleosome remodeling ATPase ISWI. *Nucleic Acids Res.*, **30**, 649–655.
30. Kornberg,R.D., LaPointe,J.W. and Lorch,Y. (1989) Preparation of nucleosomes and chromatin. *Methods Enzymol.*, **170**, 3–14.
31. Luger,K., Rechsteiner,T.J. and Richmond,T.J. (1999) Preparation of nucleosome core particle from recombinant histones. *Methods Enzymol.*, **304**, 3–19.
32. Eskeland,R., Czermin,B., Boeke,J., Bonaldi,T., Regula,J.T. and Imhof,A. (2004) The N-terminus of *Drosophila* SU(VAR)3–9 mediates dimerization and regulates its methyltransferase activity. *Biochemistry*, **43**, 3740–3749.
33. Taipale,M., Rea,S., Richter,K., Vilar,A., Lichter,P., Imhof,A. and Akhtar,A. (2005) hMOF histone acetyltransferase is required for histone H4 lysine 16 acetylation in mammalian cells. *Mol. Cell. Biol.*, **25**, 6798–6810.
34. Bonaldi,T., Regula,J.T. and Imhof,A. (2004) The use of mass spectrometry for the analysis of histone modifications. *Methods Enzymol.*, **377**, 111–130.
35. Greiner,D., Bonaldi,T., Eskeland,R., Roemer,E. and Imhof,A. (2005) Identification of a specific inhibitor of the histone methyltransferase SU(VAR)3–9. *Nature Chem. Biol.*, **1**, 143–145.
36. Bialecki,M., Shilton,A., Fichtenberg,C., Segraves,W.A. and Thummel,C.S. (2002) Loss of the ecdysteroid-inducible E75A orphan nuclear receptor uncouples molting from metamorphosis in *Drosophila*. *Dev. Cell*, **3**, 209–220.
37. Huang,N., vom Baur,E., Garnier,J.M., Lerouge,T., Vonesch,J.L., Lutz,Y., Chambon,P. and Losson,R. (1998) Two distinct nuclear receptor interaction domains in NSD1, a novel SET protein that exhibits characteristics of both corepressors and coactivators. *EMBO J.*, **17**, 3398–3412.
38. Rea,S., Eisenhaber,F., O'Carroll,D., Strahl,B.D., Sun,Z.W., Schmid,M., Opravil,S., Mechtler,K., Ponting,C.P., Allis,C.D. *et al.* (2000) Regulation of chromatin structure by site-specific histone H3 methyltransferases. *Nature*, **406**, 593–599.
39. Mosavi,L.K., Cammett,T.J., Desrosiers,D.C. and Peng,Z.Y. (2004) The ankyrin repeat as molecular architecture for protein recognition. *Protein Sci.*, **13**, 1435–1448.
40. Reeves,R. (2000) Structure and function of the HMGI(Y) family of architectural transcription factors. *Environ. Health Perspect.*, **108**, 803–809.
41. Aravind,L. and Landsman,D. (1998) AT-hook motifs identified in a wide variety of DNA-binding proteins. *Nucleic Acids Res.*, **26**, 4413–4421.
42. Tachibana,M., Sugimoto,K., Fukushima,T. and Shinkai,Y. (2001) Set domain-containing protein, G9a, is a novel lysine-preferring mammalian histone methyltransferase with hyperactivity and specific selectivity to lysines 9 and 27 of histone H3. *J. Biol. Chem.*, **276**, 25309–25317.
43. Patnaik,D., Chin,H.G., Esteve,P.O., Benner,J., Jacobsen,S.E. and Pradhan,S. (2004) Substrate specificity and kinetic mechanism of mammalian G9a histone H3 methyltransferase. *J. Biol. Chem.*, **279**, 53248–53258.
44. Collins,R.E., Tachibana,M., Tamaru,H., Smith,K.M., Jia,D., Zhang,X., Selker,E.U., Shinkai,Y. and Cheng,X. (2005) *In vitro* and *in vivo* analyses of a Phe/Tyr switch controlling product specificity of histone lysine methyltransferases. *J. Biol. Chem.*, **280**, 5563–5570.
45. Fang,J., Feng,Q., Ketel,C.S., Wang,H., Cao,R., Xia,L., Erdjument-Bromage,H., Tempst,P., Simon,J.A. and Zhang,Y. (2002) Purification and functional characterization of SET8, a nucleosomal histone H4-lysine 20-specific methyltransferase. *Curr. Biol.*, **12**, 1086–1099.
46. Rice,J.C., Nishioka,K., Sarma,K., Steward,R., Reinberg,D. and Allis,C.D. (2002) Mitotic-specific methylation of histone H4 Lys 20 follows increased PR-Set7 expression and its localization to mitotic chromosomes. *Genes Dev.*, **16**, 2225–2230.
47. Beisel,C., Imhof,A., Greene,J., Kremmer,E. and Sauer,F. (2002) Histone methylation by the *Drosophila* epigenetic transcriptional regulator Ash1. *Nature*, **419**, 857–862.
48. Schotta,G., Lachner,M., Sarma,K., Ebert,A., Sengupta,R., Reuter,G., Reinberg,D. and Jenuwein,T. (2004) A silencing pathway to induce H3–K9 and H4–K20 trimethylation at constitutive heterochromatin. *Genes Dev.*, **18**, 1251–1262.
49. Chin,H.G., Pradhan,M., Esteve,P.O., Patnaik,D., Evans,T.C. Jr and Pradhan,S. (2005) Sequence specificity and role of proximal amino acids of the histone H3 tail on catalysis of murine G9A lysine 9 histone H3 methyltransferase. *Biochemistry*, **44**, 12998–13006.
50. Gates,J., Lam,G., Ortiz,J.A., Losson,R. and Thummel,C.S. (2004) Rigor mortis encodes a novel nuclear receptor interacting protein required for ecdysone signaling during *Drosophila* larval development. *Development*, **131**, 25–36.
51. D'Avino,P.P. and Thummel,C.S. (2000) The ecdysone regulatory pathway controls wing morphogenesis and integrin expression during *Drosophila* metamorphosis. *Dev. Biol.*, **220**, 211–224.
52. Ebert,A., Schotta,G., Lein,S., Kubicek,S., Krauss,V., Jenuwein,T. and Reuter,G. (2004) Su(var) genes regulate the balance between euchromatin and heterochromatin in *Drosophila*. *Genes Dev.*, **18**, 2973–2983.
53. Edgar,B.A. and Orr-Weaver,T.L. (2001) Endoreplication cell cycles: more for less. *Cell*, **105**, 297–306.

54. Liu,L.P., Ni,J.Q., Shi,Y.D., Oakeley,E.J. and Sun,F.L. (2005) Sex-specific role of *Drosophila melanogaster* HP1 in regulating chromatin structure and gene transcription. *Nat. Genet.*, **37**, 1361–1366.
55. Beckstead,R., Ortiz,J.A., Sanchez,C., Prokopenko,S.N., Chambon,P., Losson,R. and Bellen,H.J. (2001) Bonus, a *Drosophila* homolog of TIF1 proteins, interacts with nuclear receptors and can inhibit betaFTZ-F1-dependent transcription. *Mol. Cell*, **7**, 753–765.
56. King-Jones,K. and Thummel,C.S. (2005) Nuclear receptors—a perspective from *Drosophila*. *Nature Rev. Genet.*, **6**, 311–323.
57. Badenhorst,P., Xiao,H., Cherbas,L., Kwon,S.Y., Voas,M., Rebay,I., Cherbas,P. and Wu,C. (2005) The *Drosophila* nucleosome remodeling factor NURF is required for Ecdysteroid signaling and metamorphosis. *Genes Dev.*, **19**, 2540–2545.
58. Irving,P., Ubeda,J.M., Doucet,D., Troxler,L., Lagueux,M., Zachary,D., Hoffmann,J.A., Hetru,C. and Meister,M. (2005) New insights into *Drosophila* larval haemocyte functions through genome-wide analysis. *Cell Microbiol.*, **7**, 335–350.
59. Meister,M. and Lagueux,M. (2003) *Drosophila* blood cells. *Cell Microbiol.*, **5**, 573–580.
60. Lee,D.Y., Northrop,J.P., Kuo,M.H. and Stallcup,M.R. (2006) Histone H3 lysine 9 methyltransferase G9a is a transcriptional coactivator for nuclear receptors. *J. Biol. Chem.*, **281**, 8476–8485.
61. Ashburner,M., Chihara,C., Meltzer,P. and Richards,G. (1974) Temporal control of puffing activity in polytene chromosomes. *Cold Spring Harb. Symp. Quant. Biol.*, **38**, 655–662.
62. Vakoc,C.R., Mandat,S.A., Olenchock,B.A. and Blobel,G.A. (2005) Histone H3 lysine 9 methylation and HP1gamma are associated with transcription elongation through mammalian chromatin. *Mol. Cell*, **19**, 381–391.
63. Gyory,I., Wu,J., Fejer,G., Seto,E. and Wright,K.L. (2004) PRDI-BF1 recruits the histone H3 methyltransferase G9a in transcriptional silencing. *Nature Immunol.*, **5**, 299–308.
64. Nishio,H. and Walsh,M.J. (2004) CCAAT displacement protein/cut homolog recruits G9a histone lysine methyltransferase to repress transcription. *Proc. Natl Acad. Sci. USA*, **101**, 11257–11262.
65. Roopra,A., Qazi,R., Schoenike,B., Daley,T.J. and Morrison,J.F. (2004) Localized domains of G9a-mediated histone methylation are required for silencing of neuronal genes. *Mol. Cell*, **14**, 727–738.
66. Ueda,J., Tachibana,M., Ikura,T. and Shinkai,Y. (2006) Zinc finger protein wiz links G9a/GLP histone methyltransferases to the co-repressor molecule CtBP. *J. Biol. Chem.*, **281**, 20120–20128.
67. Rayasam,G.V., Wendling,O., Angrand,P.O., Mark,M., Niederreither,K., Song,L., Lerouge,T., Hager,G.L., Chambon,P. and Losson,R. (2003) NSD1 is essential for early post-implantation development and has a catalytically active SET domain. *EMBO J.*, **22**, 3153–3163.
68. Mis,J., Ner,S.S. and Grigliatti,T.A. (2006) Identification of three histone methyltransferases in *Drosophila*: dG9a is a suppressor of PEV and is required for gene silencing. *Mol. Genet. Genomics*, **275**, 513–526.